

Permeability, Diffusivity, and Solubility of Dried Gases in Alginic Acid, Sodium Alginate, and Ammonium Alginate Self-Standing Membranes

Hiroki TAKACHI*, Takahiro HORI*, Sky AMAKAWA*, and Kazukiyo NAGAI*†

Biomass plastics are attracting research attention owing to the growing environmental problems caused by plastic products. In this study, we investigated the effects of counter cations on the gas-permeation properties of hydrogen, oxygen, nitrogen, carbon dioxide, and methane in the membrane state of alginic acid (Alg) and sodium alginate (Na-Alg), in which the hydrogen atom of the carboxy group of Alg from seaweed is replaced with sodium, as well as ammonium alginate (NH₄-Alg), in which it is replaced with ammonium ions. These polysaccharide membranes exhibited permeation behavior based on a solution-diffusion mechanism similar to that of common polymeric membranes. Using Alg as the standard, the counter cations in the Na-Alg and NH₄-Alg membranes affected the aggregation structure of the polymer chains and contributed to the construction of a densely packed membrane structure. These polysaccharide membranes can be used as gas-barrier layers for earth-friendly industrial applications such as packaging.

Keywords: Alginic acid, Alginates, Polysaccharides, Gas permeability, Solution-diffusion mechanism

1. Introduction

Plastics, which are used in wide-ranging fields including packaging materials, are chemically synthesized from fossil fuel. On the basis of the production volume of fossil fuels in 2020, the number of years fossil fuel can be extracted is estimated to be 53.5 years, so securing stable fossil-fuel resources and searching for alternative resources have become urgent issues¹⁾. One solution to this problem is to utilize biomass plastic by using biomass resources, which are non-depletable resources, as raw materials. The use of biomass resources as raw materials is expected to eliminate resource depletion. It can also uppress the increase of CO₂ in the atmosphere through the carbon cycle via biomass resources, on the basis of

carbon neutrality. However, most of the biomass resources currently used are produced on land, such as corn, which is difficult to procure because of land-area issues.

This work focused on alginic acid (Alg) and alginates in seaweeds, which can be produced at sea. In the case of *Undaria pinnatifida*, commonly known as wakame in Japan, the content of alginates in seaweeds reportedly reaches more than 50% by dry weight²). As part of our studies on food supplements, food additives, and packaging materials, our research group has been investigating natural polysaccharides, such as hyaluronic acid, sodium hyaluronate, starch, chitin, chitosan, Alg, sodium alginate (Na-Alg), calcium Alg, (Ca-Alg), ammonium alginate (NH₄-

Tel: +81-44-934-7211, E-mail: nagai@meiji.ac.jp

^{*} Department of Applied Chemistry, Meiji University

[†] Corresponding author: Kazukiyo NAGAI, 1-1-1 Higashi-mita, Tama-ku, Kawasaki 214-8571, Japan,

Alg), and λ -carrageenan, κ -carrageenan, and ι -carrageenan. The effects of the number and position of the counter cations and substituents and the helix structure of the polymer chains on water-vapor sorption properties have been studied³⁻⁶).

Literature search reveals articles in which the permeability coefficient is given only for oxygen in the presence of water vapor. For example, samples are Na-Alg and NH₄-Alg coated layers on polyethylene terephthalate films, blends of pullulan and Na-Alg, nanocomposites of cellulose nanocrystals and Na-Alg, and Alg with plasticizer^{7–10)}. However, the original permeation behavior of Alg, Na-Alg, and NH₄-Alg is unknown because the samples are not single materials and the gas is only one type, (i.e., oxygen). The effect of water vapor on the permeability of oxygen is added to the permeability of the samples.

In the preparatory experiments for the present study, self-standing membranes of Alg, Na-Alg, and NH₄-Alg were able to be manufactured, and these membranes exhibited gas-barrier properties. They can be utilized as gas-barrier layers for earth-friendly industrial applications such as packaging. The Ca-Alg membrane was too fragile to withstand the permeation experiments. Fig. 1 shows the chemical structures of Alg, Na-Alg, and NH₄-Alg. The difference among them was the counter cation acting on the carboxyl group. We further investigated the permeability, diffusivity, and solubility of dried five gases, hydrogen (H₂), oxygen (O₂), nitrogen (N₂), carbon dioxide (CO₂), and methane (CH₄), in Alg, Na-Alg, and NH₄-Alg selfstanding membranes in the dry state in terms of differences in the counter cations.

2. Experiment

2.1 Materials and membrane preparation

Powdered samples were purchased from Sigma–Aldrich LLC for Alg (CAS Registry No. 9005-32-7, Lot No. SLBV4182) and from FUJIFILM Wako Pure Chemical Corporation for Wako first-grade Na-Alg (80–120 cp, CAS Registry No. 9005-38-3, Lot No. WDN5480) and NH₄-Alg (CAS Registry No. 9005-34-5, Lot No. SAM5490).

Alg swells in water but is insoluble, so the

Fig. 1. Chemical structures of alginic acid (Alg), sodiu alginate (Na-Alg), and ammonium alginate (NH₄-Alg).

membrane was formed by a method similar to solvent casting. First, Alg powder was mixed with ultrapure water to 13 wt% of Alg powder and stirred at room temperature for 24 h to fully swell the Alg powder. Given that air was entrained by stirring and became bubbles, the Alg powder was allowed to stand for 24 h from this point to defoam. The Alg swollen with ultrapure water was then cast onto a glass plate. Membrane thickness was adjusted using a horizontal spatula, after which the water was evaporated at room temperature for 144 h. Further vacuum drying was performed at room temperature for 96 h to remove residual solvent. Membranes with dry thicknesses ranging from 590 µm to 690 µm were used in the experiments. The thickness was enough to determine the timelag of all gases in the gas-permeation measurements.

Given that Na-Alg and NH₄-Alg are soluble in water, the membranes were formed by solvent casting by using ultrapure water. For Na-Alg and NH₄-Alg, aqueous solutions were prepared at 0.75 wt% for each powder and stirred at room temperature for 24 h to obtain a solution that was uniform. The solution was passed through Kiriyama filter paper No. 5B to remove any solid impurities that may have remained during powder production. The solution was allowed to stand for 24 h to defoam because air had become entrapped in the solution and formed bubbles. The solution was then cast onto a glass Petri dish and allowed to evaporate water at 40°C and ambient pressure for 120 h. The solution was then vacuum dried at room temperature for 96 h to remove residual solvent. Membranes with dry thicknesses ranging from 60 µm to 100 µm were used in the experiments. The thickness was enough to determine the timelag of all gases in the gas-permeation measurements.

2.2 Characterization

Wide-angle X-ray diffraction (WAXD) patterns of the prepared membranes were obtained on a Rigaku 2200 Corporation RINT Ultima-III diffractometer with a tube sphere Cu-Ka. The X wavelength was 1.54 Å, sampling width was 0.02°, tube voltage was 40 kV, tube current was 40 mA, scanning angle was 2.00°/min, start angle was 5.00°, end angle was 45.00°, divergence slit was 2/3°, scattering slit was 2/3°, receiving slit was 0.3 mm, integration frequency was 1 time, and measurement temperature was 23 \pm 1°C. The d-spacing, which indicates the gap between polymer chains in the membrane, was calculated from Bragg's Equation (1). $\lambda = 2d \sin \theta$ (1)

where λ (Å) is the X-ray wavelength, θ (°) is the irradiation angle, and d (Å) is the lattice-spacing distance.

Optical microscopy (OM) observations were conducted on the prepared membranes. OM analysis was conducted using an Olympus BX-51 (Olympus Inc., Tokyo Japan). Polarized optical microscopy (POM) observations were made using an Olympus BX-51 polarization microscope (Olympus Inc., Tokyo, Japan) under cross-Nicol condition. Polarization

images were observed under additive color at 530 nm with a sensitive color plate.

Membrane-density measurements for Alg, Na-Alg, and NH₄-Alg membranes were calculated using Equation (2) by measuring the mass and volume of the membranes.

$$\rho_{membrane} = \frac{m_{membrane}}{V_{membrane}}$$
 (2)

where V_{membrane} (cm³) is the volume of the membrane.

2.3 Gas-permeation measurements

The gas permeability coefficient of pure gas H_2 , CO_2 , O_2 , N_2 , and CH_4 was determined by the constantvolume variable-pressure method at 35 ± 1 °C with reference to literature¹¹). The upstream pressure was maintained at approximately 76 ± 1 cmHg (p), whereas the downstream pressure was maintained in a vacuum. The permeability coefficient, P (cm³(STP) cm/(cm² s cmHg)), was determined by Equation (3).

$$P = \frac{dp}{dt} \frac{273V}{760(273+T)} \frac{1}{A} \frac{1}{p} l \qquad (3)$$

where dp/dt is the pressure increase over time at steady-state conditions, V (cm³) is the downstream volume, T (°C) is the temperature, l (cm) is the thickness of the membrane, A (cm²) is the membrane area, and p (cmHg) is the upstream pressure.

The apparent gas diffusion coefficient, D (cm²/s), was determined from timelag (θ). This variable was the period of time needed to reach the steady state and was calculated using Equation (4).

$$D = \frac{l^2}{60} \qquad (4)$$

According to the solution-diffusion mechanism, the apparent gas solubility coefficient, S (cm³(STP)/cm³ cmHg), can be evaluated from the following Equation (5) 12).

$$S = \frac{P}{P} \qquad (5)$$

The physical properties of the gases were obtained from data in literature¹³⁾.

3. Results and discussion

3.1 Structure of membranes

The prepared membranes were pale yellow for Alg, colorless and transparent for Na-Alg, and pale yellow

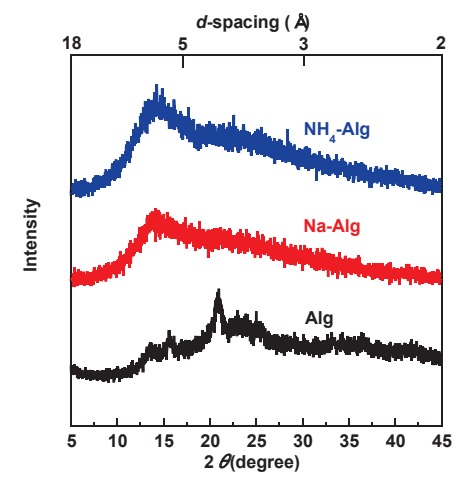
and transparent for NH₄-Alg. Fourier transform infrared absorption spectra were obtained to confirm that no change occurred in the chemical structure shown in Fig. 1 before and after membrane formation.

Fig. 2 shows the WAXD patterns of the Alg, Na-Alg, and NH₄-Alg membranes. A broad pattern with a top at $2\theta = 23^{\circ}$ –25° was observed over a wide range of $2\theta = 10^{\circ}$ –40° for the Alg membrane. Here sharp patterns were obtained in three locations at $2\theta = 13^{\circ}$ –15°, 15°–17°, and 20°–23°. For Na-Alg and NH₄-Alg membranes, broad patterns with tops at $2\theta = 13^{\circ}$ –15° were observed over a wide range of $2\theta = 10^{\circ}$ –40°. A broad shoulder peak with a top at $2\theta = 20^{\circ}$ –23° was obtained.

Fig. 3 shows the OM and POM images of the Alg, Na-Alg, and NH₄-Alg membranes. Polarization was observed in the Alg membrane, indicating a crystalline structure. Polarization was not observed in the Na-Alg and NH₄-Alg membranes, indicating an amorphous structure. The sharp pattern of the Alg membrane in Fig. 2 was consistent with that of the double-helix structure⁴). The crystallinity was 8%. The top peak positions of the Na-Alg and NH₄-Alg membranes were consistent with the pattern of the double-helix structure. The membranes were in an amorphous state with a disordered crystalline structural arrangement while maintaining the spacing of the double-helix structure.

3.2 Gas permeability, diffusivity, and solubility

Table 1 shows the permeability coefficients, diffusion coefficients, and solubility coefficients of the five gases for the Alg, Na-Alg and NH4-Alg membranes. The CH4 of NH4-Alg was smaller than 0.001×10^{-10} (cm³(STP) cm/(cm² s cmHg)) because the gas permeability coefficient was low. It cannot be measured considering that it exceeded the measurement limit of the instrument. For example, polyethylene (density 0.96 g/cm³), poly(ethylene terephthalate) (PET; semicrystalline, dependent on crystallinity), and poly(vinylidene chloride) (PVDC) at 23 °C–25 °C and a feed pressure of 1 atm had gas permeability coefficients of 0.3– 0.7×10^{-10} , 0.018– 0.035×10^{-10} , and 0.0053×10^{-10} (cm³(STP) cm/



ig. 2. WAXD patterns of Alg, Na-Alg, and NH₄-Alg membranes.

membranes	OM image (× 1,000)	POM image (× 1,000)	
Alg	5 _{Jum}	5 <u>u</u> n	
Na-Alg	5 μm	5 μm	
NH₄-Alg	5 µm	5 μm	

Fig. 3. OM and POM images of Alg, Na-Alg, and NH₄-Alg membranes.

(cm² s cmHg)), respectively¹⁴). **Table 1** shows that Alg membranes had the same level of gas permeability as PET, and the Na-Alg and NH₄-Alg membranes had the same level of gas permeability as PVDC.

The gas permeability of polymer membranes is generally considered by the solution-diffusion mechanism¹²⁾. To consider the difference in gas permeability of Alg, Na-Alg, and NH₄-Alg membranes, Table 1 summarizes the diffusion and solubility coefficients for each membrane, and Fig. 4 shows the relationship diagram plotting both coefficients. When gas permeability was diffusion dominated, the plot widened on the vertical axis but narrowed on the horizontal one. The opposite was true for the solution-dominated case. For hydrogen, the plots were almost the same on the vertical and horizontal axes, indicating that the effects of diffusivity and solubility were

Table 1 Gas permeability (P), diffusion (D), and solubility (S) coefficients in Alg, Na-Alg, and NH₄-Alg membranes at 35 °C

Polymer	Gas	$P \times 10^{10}$ (cm ³ (STP)cm/ (cm ² s cmHg))	$D \times 10^8$ (cm ² /s)	$S \times 10^{2}$ (cm ³ (STP)/ (cm ³ cmHg))
Alg	H_2	0.174 ± 0.038	1.98 ± 0.55	0.0879 ± 0.0074
	O_2	0.0214 ± 0.0011	0.143 ± 0.046	0.150 ± 0.056
	N_2	0.00740 ± 0.00052	0.0803 ± 0.0313	0.0922 ± 0.0194
	CO_2	0.0511 ± 0.0185	0.0639 ± 0.0265	0.800 ± 0.122
	$\mathrm{CH_4}$	0.00588 ± 0.00053	0.0267 ± 0.0121	0.220 ± 0.072
Na-Alg	H_2	0.0572 ± 0.0170	1.14 ± 0.67	0.0502 ± 0.0294
	O_2	0.00856 ± 0.00464	0.0864 ± 0.0422	0.0991 ± 0.0011
	N_2	0.00319 ± 0.00174	0.0459 ± 0.0192	0.0695 ± 0.0071
	CO_2	0.0161 ± 0.0109	0.0307 ± 0.0829	0.524 ± 0.097
	$\mathrm{CH_{4}}$	0.00270 ± 0.00133	0.0154 ± 0.0058	0.1753 ± 0.0852
NH ₄ -Alg	H ₂	0.0189 ± 0.0030	0.788 ± 0.050	0.0240 ± 0.0092
	O_2	0.00401 ± 0.00020	0.0477 ± 0.0271	0.0841 ± 0.0479
	N_2	0.00181 ± 0.00017	0.0329 ± 0.0101	0.0550 ± 0.0378
	CO_2	0.00780 ± 0.00056	0.0172 ± 0.0099	0.453 ± 0.129
	CH ₄	below 0.001	N/A	N/A

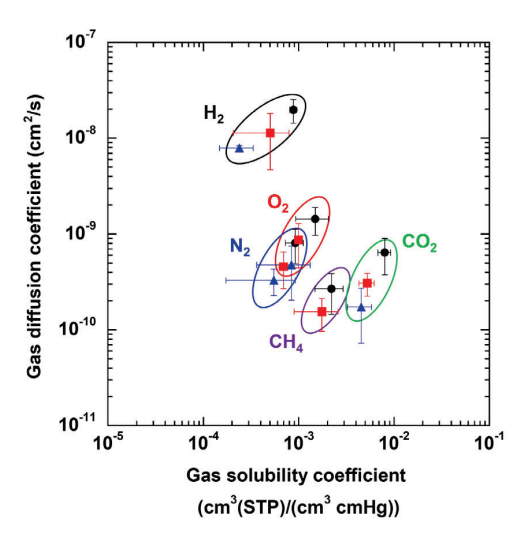


Fig. 4. Relation between gas diffusion coefficient and solubility coefficient in Alg (●), Na-Alg (■), and NH₄-Alg (▲) membranes at 35 °C.

comparable. For the other gases, the vertical and horizontal axes broadened, but the broadening on the vertical axis was larger than that on the horizontal axis, and the effect of diffusivity was slightly larger. Despite these differences, the dissimilarities in gas permeability of Alg, Na-Alg, and NH₄-Alg membranes

were not dominated by either diffusivity or solubility.

Accordingly, we proceeded to consider diffusivity and solubility. For four gases other than hydrogen, the effect of solubility was also present, but the effect of diffusivity was lightly more significant. The diffusivity of a polymer membrane is related to the size of the gas molecules. The gases used in this study were not monatomic gases, so they did not have a single molecular diameter. Therefore, the critical volume of the gas was used as the size of the gas molecules to compare the gas molecules relative to one another in three dimensions.

3.3 Properties of gas molecules

Fig. 5 plots the gas permeability coefficient, gas diffusion coefficient, and gas solubility coefficient versus the critical volume of gas. Critical volumes were obtained from data in literature¹³. The gas diffusion coefficient decreased as the critical volume of gas molecules increased for the Alg, Na-Alg and NH₄-Alg membranes. This behavior was generally observed in polymer membranes. The order of gas

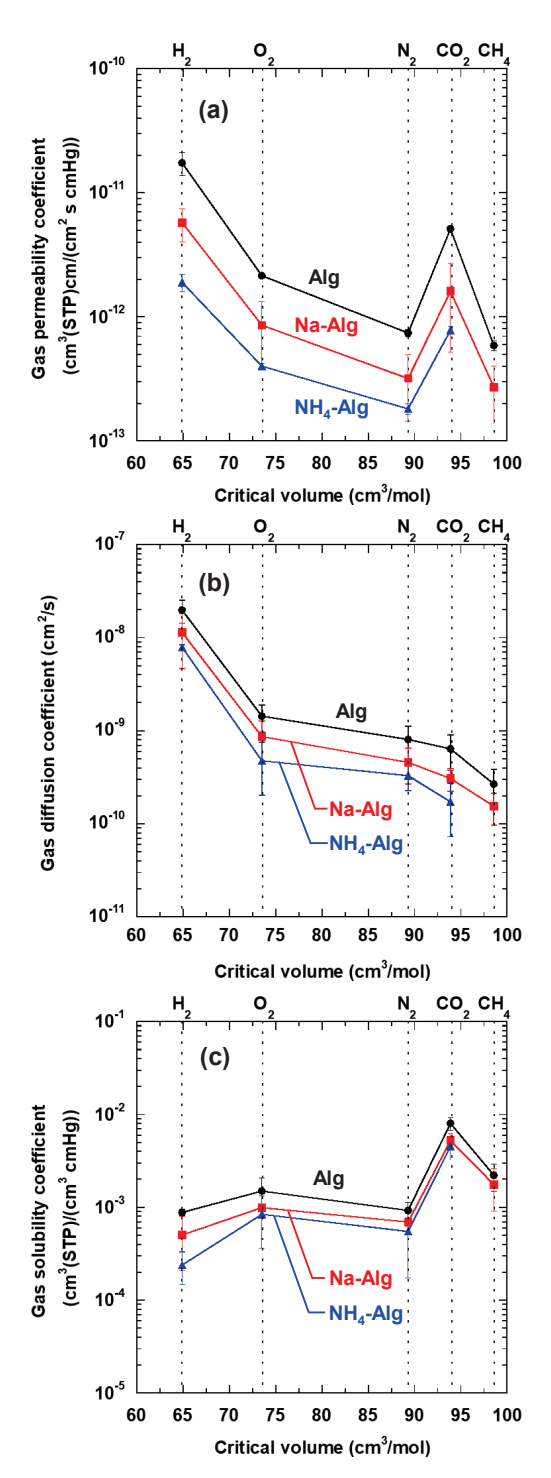


Fig. 5. (a) Gas permeability, (b) gas diffusion, and (c) as solubility coefficients versus the critical volume of gas in Alg (●), Na-Alg (■), and NH₄-Alg (▲) membranes at 35 °C.

diffusion coefficients for each gas was Alg membrane > Na-A g membrane > NH₄-Alg membrane.

Conversely the gas solubility coefficients of the Alg, Na-Alg, and NH₄-Alg membranes was not correlated with the critical volume of the gas. The order of gas solubility coefficients for each gas was Alg membrane > Na-A g membrane > NH₄-Alg membrane. The gas permeability coefficient, which was the product of the gas diffusion coefficient and the gas solubility coefficient, decreased as the critical volume of the gas molecules increased for Alg, Na-Alg, and NH₄-Alg membranes, with the exception of CO₂. The order of the gas permeability coefficient for each gas was Alg membrane > Na-Alg membrane > NH₄-Alg membrane.

The solubility of a polymer membrane was related to the condensability of gas molecules if no special interaction occurred between the functional groups of the polymer chain and the gas molecules. We used the critical temperature, which was related to the critical volume of the gas.

Fig. 6 shows the gas solubility coefficients plotted against the critical temperature of the gas. The critical temperature values were obtained from data in literature ¹³⁾. The gas solubility coefficients for the Alg, Na-Alg, and NH₄-Alg membranes increased as the critical temperature of the gas increased, that is, as the condensability of the gas molecules increased. This behavior is generally observed in polymer membranes. The order of gas solubility coefficients for each gas was Alg membrane > Na-Alg membrane > NH₄-Alg membrane.

Figs. 5 and 6 show that the gas diffusion and gas solubility coefficients of the Alg, Na-Alg, and NH₄-Alg membranes behaved in the same way as those of ordinary polymer membranes. The order of the gas permeability coefficient, gas diffusion coefficient, and gas solubility coefficient was Alg membrane > Na-Alg membrane > NH₄-Alg membrane. This order was due to the same reason as the spread of the plots in Fig. 4.

The diffusivity of gases, from the polymeric membranes' viewpoint, is related to the amount of space in the membrane. In general, fractional free volume is used. This information can be derived from calculations using the atomic group contribution method but cannot be used here because of the difficulty in properly representing the ionic bonds in

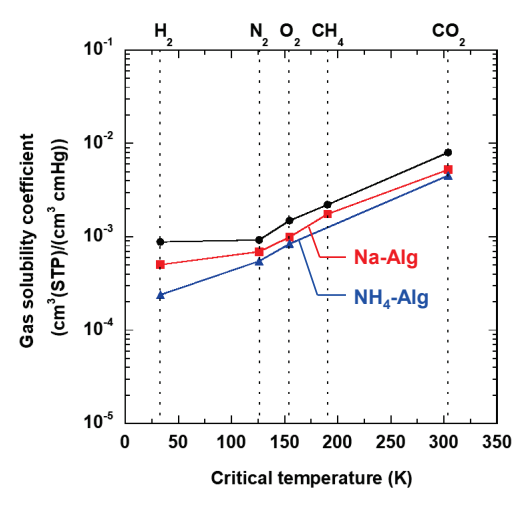


Fig. 6. Relation between gas solubility coefficient and gas critical temperature in Alg (●), Na-Alg (■), and NH₄-Alg (▲) membranes at 35 °C.

the Na-Alg and NH₄-Alg membranes. The degree of packing of the polymer chains was evident from the membrane densities, which were 1.21 ± 0.21 , 1.38 ± 0.11 , and 1.42 ± 0.08 g/cm³ for the Alg, Na-Alg, and NH₄-Alg membranes, respectively. The order of the membrane densities was consistent with the order of the gas diffusion coefficients, with sparse packing having large gas diffusion coefficients.

In the process of gas molecules entering the gap between polymer chains, they are believed to diffuse more easily if they entered from the side with a small cross-sectional area than from the side with a large cross-sectional one. Kinetic diameter is a measure of the diameter of the smallest cross-sectional area of a gas molecule. The smallest molecule is H2 that has a diameter of 2.9 Å, whereas the largest is CH₄ with a diameter of 3.8 Å. Distances in the membrane greater than 4 Å, at which the largest molecule CH₄ can diffuse, appeared in the WAXD pattern in Fig. 2. If a continuous gap between polymer chains was larger than 4 Å in the cross-sectional direction of the membrane, then all gas molecules would pass through the gap, as in a porous material. The gas diffusion coefficient would also not depend on the order of the size of gas molecules. This phenomenon implied a narrow polymer chain gap in the cross-sectional direction of the membrane that served as a bottleneck.

Gas solubility, from the polymer membrane's perspective, is related to the sum of the attraction and repulsion between the functional groups of the

polymer chain and the gas molecules. However, the forces of attraction and repulsion were difficult to measure. One indicator was the solubility parameter, which was found to be 40.8, 52.3, and 48.9 MPa^{1/2} for the Alg, Na-Alg, and NH₄-Alg membranes, respectively⁴). This trend was not consistent with the order of the gas solubility coefficients. Thus, no difference can be found from the solubility parameters.

The aggregation of the polymer chains to form a membrane demonstrated that some of the functional groups of the polymer chains contributed to the formation of the membrane. In other words, some of the functional groups of the polymer chain acted between functional groups. The interaction with the gas molecules was less than that of the free-state functional groups, and this ratio was difficult to determine. When the covalently bonded hydrogen atoms of Alg were replaced by ionically bonded Na and NH₄, the membrane density increased, i.e., packing became dense. Densification can be seen as an increase in the ratio of functional group-functional group interactions in the polymer chain. This phenomenon reduced the proportion of functional groups that interacted with gas molecules. As a result, the gas solubility coefficient decreased. In general, the hydrogen atoms of the carboxyl groups of Alg and, the -COO⁻ groups of the Na-Alg and NH₄-Alg membranes and their counter cations (Na+ and NH4+ ions) did not strongly interact with the gas molecules because of the dry state. With reference to Alg, the Na-Alg and NH₄-Alg membranes affected the aggregation structure of the polymer chains, i.e., their counter cations contributed to the construction of dense packing.

3.4 Ratio of each coefficient

We further analyzed the permeation behavior from another angle. Table 2 shows the ratios of the permeability coefficient, diffusion coefficient, and solubility coefficient of other gases to the Alg, Na-Alg, and NH₄-Alg membranes with respect to nitrogen. The nitrogen terms were all 1 for reference. For example, the ratios of oxygen to nitrogen permeability coefficients for the Alg, Na-Alg, and NH₄-Alg membranes were $2.80 \pm 1.29, 2.69 \pm 0.01$, and 2.22 ± 0.10 , respectively. The order was Alg membrane >

Table 2 Ratios of permeability, diffusion, and solubility coefficients of gases over nitrogen in Alg, Na-Alg, and NH₄-Alg membranes at $35\,^{\circ}\text{C}$

Polymer	Gas	$P(Gas)/P(N_2)$	$D(Gas)/D(N_2)$	$S(Gas)/S(N_2)$
Alg	H_2	23.3 ± 3.44	25.9 ± 3.2	0.980 ± 0.126
	O_2	2.80 ± 1.29	1.84 ± 0.14	1.56 ± 0.28
	N_2	1		1
	CO_2	6.92 ± 0.24	0.787 ± 0.023	8.79 ± 0.53
	$\mathrm{CH_4}$	0.793 ± 0.017	0.323 ± 0.025	2.33 ± 0.29
Na-Alg	H_2	21.4 ± 6.3	22.7 ± 5.1	0.686 ± 0.353
	O_2	2.69 ± 0.01	1.82 ± 0.16	1.44 ± 0.13
	N_2	1		1
	CO_2	4.53 ± 0.95	0.719 ± 0.120	7.48 ± 0.62
	$\mathrm{CH_4}$	0.881 ± 0.064	0.342 ± 0.017	2.42 ± 0.98
NH ₄ -Alg	H_2	10.4 ± 0.7	25.9 ± 6.5	0.609 ± 0.252
	O_2	2.22 ± 0.10	1.32 ± 0.43	1.76 ± 0.34
	N_2	1		1
	CO_2	4.32 ± 0.10	0.475 ± 0.156	12.6 ± 6.3
	CH ₄	below 0.5	N/A	N/A

Na-Alg membrane > NH₄-Alg membrane, and the difference in permeability coefficient decreased. The order was similar to those of hydrogen, carbon dioxide, and methane. In general, the upper bound trend between gas selectivity (i.e., small gas-to-large gas ratio) and gas permeability demonstrated that low gas permeable polymers had high gas selectivity and vice versa¹²⁾. Low gas permeable polymers also tended to have high density and low fractional free volume. Table 2 shows the opposite trend to the general behavior of polymeric membranes; that is, the small gas-to-large gas ratios were small for low gas permeable polymers. To consider the reason for this phenomenon, the ratio of the diffusion coefficient to the solubility coefficient was examined.

In terms of the ratio of diffusion coefficients, excluding hydrogen in the NH₄-Alg membrane, the difference decreased in the order Alg membrane > Na-Alg membrane > NH₄-Alg membrane. Conversely, when oxygen and carbon dioxide were excluded from the Na-Alg membrane, the difference in the solubility coefficient ratio increased in the order of Alg

membrane < Na-Alg membrane < NH₄-Alg membrane. Considering the order of the ratio of permeability coefficients, the ratio of diffusion coefficients was more dominant than the ratio of solubility coefficients. A small ratio of diffusion coefficients meant that the sieving action of gas molecules decreased. The structure in which the hydrogen atoms of Alg were replaced by Na⁺ or NH₄⁺ ions resulted in dense packing. The outcome was an aggregated structure of polymer chains that reduced the sieving effect of the diffusion pathway. However, identifying this structure is impossible with the current scientific technology.

4. Conclusion

The effect of counter cations on the gas permeation properties of Alg, Na-Alg, and NH₄-Alg self-standing membranes was investigated. These polysaccharide membranes exhibited gas permeation, diffusion, and solubility behavior similar to those of common polymeric membranes. The differences in gas permeability were the effects of gas diffusivity and gas solubility factors and owing to variations in the

packing structure of the polymer chains. The different counter cations produced different polymer chain arrangements and altered the packing state of the membranes. If an industrially appropriate method of membrane formation can be obtained, we believe that the membranes can be serve gas-barrier layers for earth-friendly industrial applications such as packaging.

Acknowledgments

This research was partially supported by a Grant-inaid for Scientific Research C (18K04757, 21K04698) from the Ministry of Education, Culture, Sports, Science and Technology, Japan, the Japanese Society of the Promotion of Science.

References

- METI Agency Natural Resources and Energy, Cabinet Decision Made on the FY2022 Annual Report on Energy (Japan's Energy White Paper 2023).
- A. Skriptsova, V. Khomenko, and V. Isakov, Seasonal changes in growth rate, morphology and alginate content in *Undaria pinnatifida* at the northern limit in the Sea of Japan, J. Appl. Phycol. 16 p.17 (2004).
- N. Shimanuki and K. Nagai, Effects of substituents on water vapor sorption in liquidwater-soluble polysaccharides, J. Appl. Polym. Sci. 136 p.48223 (2019).
- N. Shimanuki, M. Imai, and K. Nagai, Effects of counter cations on the water vapor sorption properties of alginic acid and alginates, J. Appl. Polym. Sci. 137 p.49326 (2020).
- N. Hirota and K. Nagai, Helical structures and water vapor sorption properties of carrageenan membranes derived from red algae, Carbohydr. Polym. Technol. Appl. 3 p.100200 (2022).
- R. Nishida, N. Hirota, and K. Nagai, Anti-cluster behavior and its mechanism during water vapor

- sorption in chitin and chitosan membranes, Carbohydr. Polym. Technol. Appl. 5 p.100312 (2023).
- Y. Kato, J. Kaminaga, R. Matsuo, and A. Isogai, Oxygen Permeability and Biodegradability of Polyuronic Acids Prepared from Polysaccharides by TEMPO-Mediated Oxidation, J. Polym. Environ. 13 p.261 (2005).
- G. Lavrič, A. Oberlintner, I. Filipova, U. Novak,
 B. Likozar, and U. Vrabič-Brodnjak, Functional Nanocellulose, Alginate and Chitosan Nanocomposites Designed as Active Film Packaging Materials, Polymers. 13 p.2523 (2021).
- V. Jost, K. Kobsik, M. Schmid, and K. Noller, Influence of plasticiser on the barrier, mechanical and grease resistance properties of alginate cast films, Carbohydr. Polym. 110 p.309 (2014).
- Q. Xiao, K. Lu, Q. Tong, and C. Liu, Barrier Properties and Microstructure of Pullulan– Alginate-Based Films, J. Food Process Eng. 38 p.155 (2015).
- 11) T. Ito, R. Shiota, N. Taniguchi, R. J. Spontak, and K. Nagai, Gas-separation and physical properties of ABA triblock copolymers synthesized from polyimide and hydrophilic adamantane derivatives, Polymer 202 p.122642 (2020).
- 12) R.W. Baker, Membrane Technology and Applications, McGraw-Hill, p.15 (2000).
- B.E. Poling, J.M. Prausnitz, J.P. O'Connell, The Properties of Gases and Liquids, Fifth ed., McGraw-Hill, p.2 (2001).
- 14) W.J. Koros, C.M. Zimmerman, Transport and Barrier Properties, in R.F. Brady Ed., Comprehensive Desk Reference of Polymer Characterization and Analysis, American chemical Society, p. 680 (2003).

(Received: 17 June 2024) (Accepted: 27 August 2024)